

# Small amplitude thermocapillary flow and surface deformations in a liquid bridge

H. Kuhlmann<sup>a)</sup>

Department of Mechanical and Aerospace Engineering, Arizona State University, Tempe, Arizona 85287

(Received 30 August 1988; accepted 30 November 1988)

A cylindrical liquid bridge under asymmetric heating is investigated for small Reynolds, Prandtl, and capillary numbers. Flow field and surface deformation are calculated in terms of a Papkovitch–Fadle series. The present analytical solution is in very good agreement with recent numerical results. A comparison with numerical simulations of the full Navier–Stokes equations without surface deformations is made.

## I. INTRODUCTION

With the increased importance of high quality semiconductor single crystals, a great deal of research effort has focused on the study of fluid flows in molten phases during crystal growth processes.<sup>1</sup> In particular, the containerless float-zone process has received much attention, this attention being stimulated by discussions about its application in a microgravity environment. Under low gravity, or in small liquid volumes, the flow is mainly driven by temperature induced surface tension gradients (thermocapillary convection). These flows are of fundamental importance in crystal growth because they are known to become unstable, leading to a degradation of crystal quality. Since the real float-zone system involves many detailed complications such as moving melting and solidification fronts, model systems play an important role in experimental,<sup>2–4</sup> numerical,<sup>5–9</sup> and theoretical<sup>10–16</sup> studies of the most important physical effects in the melt.

A very useful system for studying thermocapillary phenomena in a float-zone consists of a liquid bridge between two concentric cylindrical rods held at different temperatures, where the fluid motion is driven by surface tension gradients along the free surface.<sup>8</sup> Although experimental and numerical progress has been made in determining the structure and stability range of the basic, steady, axisymmetric flow, only a few analytical results are available for a bridge of finite length. Bauer<sup>10</sup> discussed the influence of the aspect ratio (length/radius) on the flow structure by considering periodic free boundaries in the axial direction and an axially periodic heat load. He obtained results for small Reynolds numbers and zero gravity using an axial Fourier analysis. Xu and Davis<sup>14</sup> investigated the leading order core flow in a long liquid zone. For large mean surface tension they obtained similarity solutions, which depend only on the imposed temperature distribution on the free surface. These results hold for arbitrarily large driving, i.e., for unlimited Reynolds number. Planar systems have also been studied<sup>11–13</sup> to analyze thermocapillary flow. All theoretical investigations of the stability of the basic states against time dependent oscillatory flow in both planar and cylindrical geometries have been carried out for infinitely large systems,<sup>12,15</sup> thus dealing with the instability mechanisms,<sup>16</sup> but neglecting the considerable stabilizing effect of the rigid boundaries.

<sup>a)</sup> Present address: FR 11.1 Theoretische Physik, Universität Saarbrücken, 6600 Saarbrücken, Federal Republic of Germany.

Recently Rybicki and Floryan<sup>8,9</sup> numerically investigated the flow structure and free surface deformations of a cylindrical zone for both small Reynolds and zero Prandtl numbers in the absence of gravity. The influence of different heat loads, aspect ratios, and end conditions has been discussed in great detail. Their basic results are recovered by the present work. Here, however, an analytical rather than numerical approach is made. Moreover, the convective effect on the temperature field is obtained and several limits of the aspect ratio can be examined exactly, relating the present findings to results for both infinitely short and long zones. The analysis starts with an expansion of all fields for small Reynolds, Prandtl, and capillary numbers. An asymptotic solution is then obtained using a further expansion in terms of Papkovitch–Fadle functions. This last method has been introduced by Smith<sup>17</sup> and successfully applied to some Stokes flow problems by Joseph and Sturges,<sup>18</sup> Yoo and Joseph,<sup>19</sup> and Benmalek.<sup>20</sup>

## II. PROBLEM FORMULATION AND FIELD EXPANSION

The system under consideration is a liquid bridge of an incompressible fluid with kinematic viscosity  $\nu$ , density  $\rho$ , thermal diffusivity  $\kappa$ , and thermal expansion coefficient  $\beta$ , which is suspended between two coaxial cylindrical rods of radius  $R$  a distance  $d$  apart. The solid surfaces in contact with the liquid are planar. The liquid volume is  $V = \pi R^2 d$  and the location of the deformable liquid–gas interface is described by  $\xi(z)$ , with  $\xi(z = \pm d/2) = R$  assuming fixed contact lines (cf. Fig. 1). The liquid is heated from above by holding the upper and lower cylinders at temperatures  $T_u$  and  $T_l$ , respectively, with  $\Delta T = T_u - T_l > 0$ . Forces on the fluid are caused by the acceleration of gravity  $\mathbf{g} = -g\mathbf{e}_z$ , and by the temperature dependent surface tension, approximated linearly by

$$\sigma(T) = \sigma_0(T_0) - \gamma(T - T_0),$$

where

$$T_0 = \frac{1}{2}(T_u + T_l)$$

and  $\gamma$  is the linear coefficient of a Taylor expansion of  $\sigma$ . The ambient gas is assumed to have a linear temperature profile of  $T_a(z) = T_0 + \Delta T \cdot z/d$  at the interface.

If the temperature difference  $\Delta T$  is small, the flow and the surface deformations are steady and axisymmetric.<sup>4</sup> Therefore, the radial and axial velocities,  $u(r,z)$  and  $w(r,z)$ , respectively, and the temperature  $T(r,z)$  are governed by the

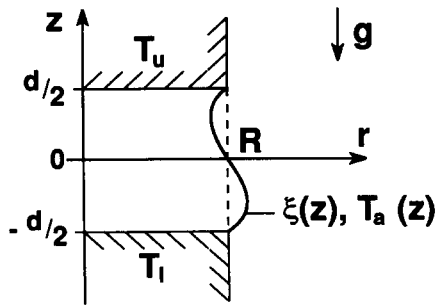


FIG. 1. Sketch of the liquid bridge.

time independent axisymmetric Navier–Stokes and energy equations, which are written in the Boussinesq approximation as

$$L^2 \psi = -Gr D\theta - [(2/r)(\partial_z \psi) + (D_* \psi) \partial_z - (\partial_z \psi) D_*] L\psi, \quad (1a)$$

$$\Delta \theta = -Pr \{ [(D_* \psi) \partial_z - (\partial_z \psi) D_*] \theta + D_* \psi \}. \quad (1b)$$

For convenience,  $\psi$  is defined such that  $u = \partial_z \psi$  and  $w = -D_* \psi$  ( $D_* = D + 1/r = \partial_r + 1/r$ ). Here, it is referred to as the “streamfunction,” although the streamlines are not given by  $\psi = \text{const}$ , as occurs for the Stokes streamfunction. Also,  $\theta$  is the nondimensional temperature deviation from the conduction profile  $T_c = T_a(z)$ , the two-dimensional Laplace operator is  $\Delta = D_* D + \partial_z^2$ , and  $L = DD_* + \partial_z^2$ . The Grashof and Prandtl numbers are denoted by  $Gr = d^3 g \beta \Delta T / \nu^2$  and  $Pr = \nu / \kappa$ , respectively, and the scales for length, time, velocity, and temperature are  $d$ ,  $d^2 / \nu$ ,  $\nu / d$ , and  $\Delta T$ , respectively.

The boundary conditions on the rigid cylinder ends are

$$\psi = \partial_z \psi = \theta = 0, \quad z = \pm \frac{1}{2}, \quad (2)$$

and the deformable surface is modeled by a free boundary with the vanishing normal and tangential stresses, respectively,

$$C [D \partial_z - \xi_z^2 D_* \partial_z - \xi_z (\partial_z^2 - DD_*)] \psi - (N^2/2) C (p - p_a) + (N/2) \text{Re} [1 - C(\theta + z)] (\xi^{-1} - \xi_{zz}/N^2) = 0, \quad (3a)$$

$$r = \xi(z)$$

and

$$\{ \partial_z^2 - DD_* + 2\xi_z D_* \partial_z + \xi_z [2D \partial_z - \xi_z (\partial_z^2 - DD_*)] \} \psi + N \text{Re} (\xi_z D \theta + \partial_z \theta + 1) = 0, \quad r = \xi(z), \quad (3b)$$

where the fluid pressure and the external pressure are denoted by  $p$  and  $p_a$ , respectively,  $\Gamma = d/R$  is the aspect ratio, and  $N = (1 + \xi_z^2)^{1/2}$ . The strength of the driving is measured by the Reynolds number  $\text{Re} = \gamma d \Delta T / \rho \nu^2$  and the capillary number  $C = \gamma \Delta T / \sigma_0$  measures the relative variation of surface tension with temperature. Moreover, the normal component of the velocity must vanish at the surface:

$$(\partial_z + \xi_z D_*) \psi = 0, \quad r = \xi(z). \quad (3c)$$

The thermal boundary condition on the interface is

$$(D - \xi_z \partial_z + BN) \theta = 0, \quad r = \xi(z), \quad (3d)$$

where the Biot number  $B = hd/\kappa$  measures the heat transfer through the surface,  $h$  being the heat transfer coefficient. Continuity along the axis  $r = 0$  requires

$$\psi = DD_* \psi = D\theta = 0, \quad r = 0. \quad (4)$$

To find the leading order contributions to the flow and temperature fields for small  $\text{Re}$ ,  $\text{Pr}$ , and  $C$ , and to obtain corrections to the static meniscus, all fields are expanded in a power series:

$$\psi(r, z) = \sum_{\substack{n=1 \\ m=0 \\ k=0}}^{\infty} \text{Re}^n \text{Pr}^m C^k \psi_{nmk}(r, z), \quad (5a)$$

$$\theta(r, z) = \sum_{\substack{n=1 \\ m=0 \\ k=0}}^{\infty} \text{Re}^n \text{Pr}^m C^k \theta_{nmk}(r, z), \quad (5b)$$

$$p(r, z) = p_a + \frac{\text{Re}}{C} p_s(z) + \sum_{\substack{n=1 \\ m=0 \\ k=0}}^{\infty} \text{Re}^n \text{Pr}^m C^k p_{nmk}(r, z), \quad (5c)$$

$$\xi(r, z) = \xi_s(z) + \sum_{\substack{n=0 \\ m=0 \\ k=1}}^{\infty} \text{Re}^n \text{Pr}^m C^k \xi_{nmk}(z). \quad (5d)$$

Inserting this expansion boundary condition [(3a)] yields, at lowest order,  $O(\text{Re}^1 \text{Pr}^0 C^0)$ , the static meniscus problem [subscript  $s$  in (5) and (6)]

$$p_s = \frac{1}{N_s} \left( \xi_s^{-1} + \frac{\partial_z^2 \xi_s}{N_s^2} \right). \quad (6)$$

In order to retain a rectangular domain for the lowest-order flow and temperature, the exact limit  $C \rightarrow 0$  or the absence of gravity ( $Gr = 0$ ) is considered. In the former case, the infinite sum in expansion (5d) drops out and surface deformations cannot occur. In both cases, however, the static zone shape is cylindrical with  $\xi_s = 1/\Gamma$ , and the pressure jump  $p_s = \Gamma$  is independent of  $z$ .

### III. ASYMPTOTIC SOLUTION

#### A. The flow and temperature field

Inserting the expansion (5) into Eqs. (1a) and (1b), and equating terms of lowest order  $O(\text{Re}^1 \text{Pr}^0 C^0)$ , one obtains

$$L^2 \psi_{100} = -Gr D\theta_{100}, \quad (7a)$$

$$\Delta \theta_{100} = 0. \quad (7b)$$

The corresponding boundary conditions of the same order, obtained from (2), (3b)–(3d), and (4), are

$$\psi_{100} = \partial_z \psi_{100} = \theta_{100} = 0, \quad z = \pm \frac{1}{2}, \quad (8a)$$

$$\psi_{100} = DD_* \psi_{100} = D\theta_{100} = 0, \quad r = 0, \quad (8b)$$

$$\psi_{100} = DD_* \psi_{100} - 1 = (D - B)\theta_{100} = 0, \quad r = 1/\Gamma. \quad (8c)$$

From this it follows that the temperature field at  $O(\text{Re}^1 \text{Pr}^0 C^0)$  is purely conducting with  $\theta_{100} = 0$ . Therefore, the leading order flow field  $\psi_{100}$  is independent of  $Gr$  and  $B$ , i.e., it is affected neither by gravity nor by the heat

transfer rate at the free surface. Thus one is left with the Stokes flow problem

$$L^2 \psi_{100} = 0. \quad (9)$$

To solve this equation with boundary conditions (8),  $\psi_{100}$  is expanded in a series of even Papkovitch–Fadle functions<sup>18</sup>  $\phi_1^{(n)}$ ,

$$\psi_{100}(r, z) = \sum_{n=-\infty}^{\infty} A_n I_1(2s_n r) \phi_1^{(n)}(z) / s_n^2, \quad (10)$$

satisfying (9) exactly.<sup>19</sup> Here,  $I_1$  is a modified Bessel function of first order, and  $s_n$  are the first quadrant roots<sup>21</sup> of

$$2s_n - \sin 2s_n = 0, \quad (11)$$

numbered according to their increasing real parts. The functions  $\phi^{(n)} = (\phi_1^{(n)}, \phi_2^{(n)})$  and  $\psi^{(n)} = (\psi_1^{(n)}, \psi_2^{(n)})$  are given by<sup>18</sup>

$$\phi_1^{(n)}(z) = s_n \sin s_n \cos 2s_n z - 2z s_n \cos s_n \sin 2s_n z, \quad (12a)$$

$$\phi_2^{(n)}(z) = -(s_n \sin s_n + 2 \cos s_n) \cos 2s_n z + 2z s_n \cos s_n \sin 2s_n z, \quad (12b)$$

$$\psi_1^{(n)}(z) = (s_n \sin s_n - 2 \cos s_n) \cos 2s_n z - 2z s_n \cos s_n \sin 2s_n z, \quad (12c)$$

$$\psi_2^{(n)}(z) = \phi_1^{(n)}(z). \quad (12d)$$

The expansion coefficients  $A_n$  are found by projecting the boundary condition (8c)

$$\begin{bmatrix} 1 \\ 0 \end{bmatrix} = \begin{bmatrix} DD_* \\ \partial_z^2 \end{bmatrix} \psi_{100} \left( \frac{1}{\Gamma} \right) = \sum_{n=-\infty}^{\infty} 4A_n I_1 \left( \frac{2s_n}{\Gamma} \right) \phi^{(n)} \quad (13)$$

onto the orthogonal vector functions  $\psi^{(m)}$  using the biorthogonality condition

$$\int_{-1/2}^{1/2} \psi^{(n)} \cdot \begin{bmatrix} 0 & -1 \\ 1 & 2 \end{bmatrix} \phi^{(n)} dz = -2 \cos^4 s_n \delta_{nm}, \quad (14)$$

where  $\delta_{nm}$  is the Kronecker symbol. This yields the  $O(\text{Re}^1 \text{Pr}^0 C^0)$  streamfunction:

$$\psi_{100}(r, z) = \lim_{N \rightarrow \infty} \sum_{n=-N}^N \frac{-1}{4s_n^2 \cos^4 s_n} \frac{I_1(2s_n r)}{I_1(2s_n/\Gamma)} \phi_1^{(n)}(z). \quad (15)$$

The velocity field corresponding to the streamfunction  $\psi_{100}$  has been calculated by direct numerical integration of the linear differential equation (9) by Rybicki and Floryan,<sup>8</sup> who also extensively discussed the respective flow patterns. For  $\Gamma \gtrsim 1$ , a single toroidal vortex exists, whereas for  $\Gamma \lesssim 0.5$  the flow separates into a radial sequence of concentric counter-rotating toroidal vortices with equal cross sections, whose intensities decay nearly exponentially as  $r \rightarrow 0$ . The boundary between adjacent vortices is not flat but takes an outward concave shape.

Having found  $\psi_{100}$ , it is easy to give the first nonvanishing correction to the conduction temperature  $\theta_{100} = 0$ . The  $O(\text{Re}^1 \text{Pr}^1 C^0)$  equations are

$$L^2 \psi_{110} = -\text{Gr} D\theta_{110}, \quad (16a)$$

$$\Delta \theta_{110} = -D_* \psi_{100}, \quad (16b)$$

with homogeneous boundary conditions like (8a)–(8c), but

with  $DD_* \psi_{110} = 0$  instead of  $DD_* \psi_{100} = 1$  at  $r = 1/\Gamma$ . The solution of Eqs. (16a) and (16b) is straightforward. For the temperature  $\theta_{110}$  one obtains

$$\theta_{110}(r, z) = \sum_{n=-\infty}^{\infty} 2a_n s_n \left[ I_0(2s_n r) (z^2 \cos 2s_n z + b_n z \sin 2s_n z + c_n \cos 2s_n z) + \sum_{k=0}^{\infty} B_{nk} I_0(\lambda_k r) \cos \lambda_k z \right], \quad (17a)$$

where

$$a_n = [16s_n^2 \cos^3 s_n I_1(2s_n/\Gamma)]^{-1}, \quad (17b)$$

$$b_n = -(1 + 2 \sin^2 s_n) / 2s_n, \quad (17c)$$

$$c_n = -\frac{1}{4}(1 + 2b_n \tan s_n), \quad (17d)$$

$$\lambda_k = (2k + 1)\pi, \quad (17e)$$

$$B_{nk} = -2 \frac{2s_n I_1(2s_n/\Gamma) + B I_0(2s_n/\Gamma)}{\lambda_k I_1(\lambda_k/\Gamma) + B I_0(\lambda_k/\Gamma)} \cdot \int_{-1/2}^{1/2} \cos \lambda_k z (z^2 \cos 2s_n z + b_n z \sin 2s_n z + c_n \cos 2s_n z) dz. \quad (17f)$$

The calculation of  $\psi_{110}$  is omitted. A corresponding calculation for a similar problem can be found in Ref. 21.

Since there is no coupling of  $\psi$  and  $\theta$  along the free surface at  $O(\text{Re}^1)$ , contributions  $\psi_{1mk}$  with  $m > 0$  and  $\theta_{1mk}$  with  $m > 1$  are due to buoyancy or deformation effects. Therefore, for  $\text{Gr} = 0$  and  $C \rightarrow 0$ , the solution has the form

$$\psi(r, z) = \text{Re} \psi_{100}(r, z) + O(\text{Re}^2), \quad (18a)$$

$$\theta(r, z) = \text{Re Pr} \theta_{110}(r, z) + O(\text{Re}^2). \quad (18b)$$

## B. Small surface deformations

The lowest order surface deformation of the liquid bridge is calculated by letting  $\text{Gr} = 0$ , and considering boundary condition (3a) for  $\xi$  at  $O(\text{Re}^1 \text{Pr}^0 C^1)$ :

$$(\partial_z^2 + \Gamma^2) \xi_{001} = -\Gamma z + (2\partial_z D\psi_{100} - p_{100})_{1/\Gamma}. \quad (19)$$

To derive this equation,  $\xi^{-1}$  had to be expanded assuming  $C |\xi_{001}| \ll 1/\Gamma$ . Moreover, Eq. (19) requires that a flow be present, i.e.,  $\text{Re} \neq 0$ . The resulting deformation  $C \xi_{001}(z)$ , however, is independent of  $\text{Re}$ , i.e., the strength of that flow, whereas the particular shape of  $\xi_{001}(z)$  is determined by the structure of the normal stresses induced by the flow at  $O(\text{Re}^1 \text{Pr}^0 C^0)$ , and by the temperature dependence of the surface tension.

After calculating  $p_{100}$  from  $Dp_{100} = \partial_z L\psi_{100}$ , Eq. (19) can be solved to obtain the asymmetric deformation

$$\xi_{001}(z) = \frac{1}{\Gamma} \left( \frac{1}{2} \frac{\sin \Gamma z}{\sin \Gamma/2} - z \right) + \sum_{n=-\infty}^{\infty} \left[ C_n \left( z \cos 2s_n z - \frac{1}{2} \frac{\sin \Gamma z}{\sin \Gamma/2} \right) + D_n \left( \sin 2s_n z - \sin s_n \frac{\sin \Gamma z}{\sin \Gamma/2} \right) \right], \quad (20a)$$

$$\Gamma/2 \neq \begin{cases} n\pi, \\ \tan \Gamma/2, \end{cases} \quad (20a)$$

with

$$C_n = \frac{4s_n}{(4s_n^2 - \Gamma^2)\cos^3 s_n} \left( \frac{\Gamma}{2s_n} - \frac{I_0(2s_n/\Gamma)}{I_1(2s_n/\Gamma)} \right), \quad (20b)$$

$$D_n = \frac{2}{(4s_n^2 - \Gamma^2)\cos^4 s_n} \times \left[ \left( s_n \sin s_n + \cos s_n - \frac{8s_n^2 \cos s_n}{4s_n^2 - \Gamma^2} \right) \cdot \left( \frac{\Gamma}{2s_n} - \frac{I_0(2s_n/\Gamma)}{I_1(2s_n/\Gamma)} \right) - \cos s_n \frac{I_0(2s_n/\Gamma)}{I_1(2s_n/\Gamma)} \right]. \quad (20c)$$

Note that the volume  $V$  is preserved at  $O(C^{-1})$ .

Aspect ratios  $\Gamma/2 = n\pi$  and  $\Gamma/2 = \tan \Gamma/2$  have been identified as bifurcation points of  $\xi_{001}$ .<sup>9</sup> However, as  $\Gamma \uparrow 2\pi$ , the solution  $\xi_{001}$  [Eqs. (20)] diverges, and the differential equation (19) loses its validity if  $C \gg O(2\pi - \Gamma)$ . The form, size, and dependence on  $\Gamma$  of the deformation  $\xi_{001}$  are identical to the results given in Ref. 9.

#### IV. GEOMETRY LIMITS

##### A. $\Gamma \rightarrow 0$

In the limit of a small gap,  $\psi_{100}(r, z)$  takes a simple form if one considers intermediate radial positions  $1 \ll r \ll 1/\Gamma$ . Then  $\psi_{100}$  is dominated by the  $n = \pm 1$  summands, so that

$$\psi_{100} \left( 1 \ll r \ll \frac{1}{\Gamma}, z \right) \simeq - \frac{(\pi s_1/\Gamma)^{1/2} \phi_1^{(1)}(z)}{2s_1^2 \cos^4 s_1} \exp \left[ 2s_1 \left( r - \frac{1}{\Gamma} \right) \right] + \text{c.c.} \quad (21)$$

Therefore, the two-dimensional flow in a radial cross section of the bulk consists of equal sized vortices with an extension  $\pi/2 \operatorname{Im}(s_1) = 1.396$ , which are damped exponentially toward  $r = 0$  with a decay constant  $2 \operatorname{Re}(s_1) = 4.212$ . These are the same values as obtained by Moffatt<sup>22</sup> for a general class of two-dimensional flows between rigid planes of infinite extent. Thus the cross-sectional diagrams are similar in both cases, but the overall flow structure consists of toroidal vortices and straight rolls, respectively. Rybicki and Floryan<sup>8</sup> have suggested this analogy numerically. Equation (21) is, in fact, a very good approximation for the vortex diameters, which is indicated by Table I, where the radial zeros of  $\psi_{100}$  [Eq. (15)] calculated using Newton's method are shown for  $\Gamma = 0.1$ . For this aspect ratio, however, the absolute radial positions of the vortices are still influenced by the finite radius of the liquid bridge.

The limiting form of the surface deformation  $\xi_{001}$  is

TABLE I. Radial zeros  $r_i$  of  $\psi_{100}(r, z = 0)$  at midplane for  $\Gamma = 0.1$ . [Truncation order (cf. Sec. V) is  $N = 20$ .]

$i$	1	2	3	4	5	6	7
$r_i$	0.046	1.714	3.115	4.513	5.910	7.306	8.702
$r_i - r_{i-1}$	...	1.668	1.401	1.398	1.397	1.396	1.396

readily obtained from (20) as

$$\xi_{001}(z, \Gamma \rightarrow 0) = \sum_{n=-\infty}^{\infty} \left( \frac{\sin 2s_n z - 2z \sin s_n}{2 \cos^5 s_n} - \frac{z \cos 2s_n z - z \cos s_n}{s_n \cos^3 s_n} \right). \quad (22)$$

This deformation has the known sinusoidal shape with extrema of size  $|\xi_{001}| = 0.0125$  at  $z = \pm 0.33$ , which is 6% less than the extrapolated value given by Rybicki and Floryan.<sup>9</sup>

##### B. $\Gamma \rightarrow \infty$

Although a liquid bridge is subject to capillary instabilities under most circumstances when  $\Gamma$  is large,<sup>9,23</sup> the limit  $\Gamma \rightarrow \infty$  and  $C \rightarrow 0$  is very useful when studying thermocapillary instabilities.<sup>15</sup> In this limit, the bulk flow is independent of  $z$  and is governed by [cf. Eqs. (1)]

$$(DD_*)^2 \psi = -Gr D\theta, \quad (23a)$$

$$D_* D\theta = -Pr D_* \psi. \quad (23b)$$

These linear equations are identical to Eqs. (9) and (16) for the expansion solution taking the limit  $\Gamma \rightarrow \infty$ . Therefore, the expansion to  $O(\operatorname{Re}^{-1} \operatorname{Pr}^{-1} C^0)$  approaches the exact solution if  $\Gamma \rightarrow \infty$  and  $C \rightarrow 0$ . For example, expanding  $\psi_{100}(r, z = 0)$  [Eq. (15)] for small  $1/\Gamma$  yields the axial velocity

$$w_{100}(r, \Gamma \rightarrow \infty) = (\Gamma/2)(1/2\Gamma^2 - r^2), \quad (24)$$

which is identical to the Hagen-Poiseuille profile given by Xu and Davis<sup>14</sup> for  $C \rightarrow 0$ .

Within the present approach it is not possible to take the formal limit of  $\xi_{001}(\Gamma \rightarrow \infty)$  because of its periodic divergence with  $\Gamma$ . Between these poles, however, there always exist intervals for which the relation  $C |\xi_{001}| \ll 1/\Gamma$  holds, so that  $\xi_{001}$  is a valid approximation to the deformation problem regardless of its stability properties.

#### V. COMPARISON WITH NONLINEAR NUMERICAL CALCULATIONS

In this section a comparison is made between the actual small  $\operatorname{Re}$ ,  $\operatorname{Pr}$ ,  $C$  approximation and numerical solutions of the full equations (1)–(4) for  $C \rightarrow 0$ . Since these numerical data do not include surface deformations, only axial velocity and temperature deviations are considered. For a practical evaluation of  $\psi_{100}$  and  $\theta_{110}$  the sums over  $n$  and  $k$  in (15) and (17) have to be truncated at orders  $N$  and  $K$ , respectively. Here  $N$  was chosen such that the results for order  $N + 1$  did not deviate from those at order  $N$  by more than about 1% of the maximum absolute value of  $w_{100}$ . Taking the same truncation order  $K = N$  for the calculation of  $\theta_{110}$  always yielded sufficient accuracy. This ensures that all values calculated at interior points are fully converged and only a small uncertainty is left for values at  $r = 1/\Gamma$ . Since the relative length of the turning zones at  $z = \pm \frac{1}{2}$  decreases as  $\Gamma$  increases, the series have to be truncated at increasing orders to obtain good convergence. Some general conditions for the convergence of Papkovitch-Fadle series can be found in Refs. 24 and 25.

The radial dependence of  $w$  and  $T$  at the midplane  $z = 0$

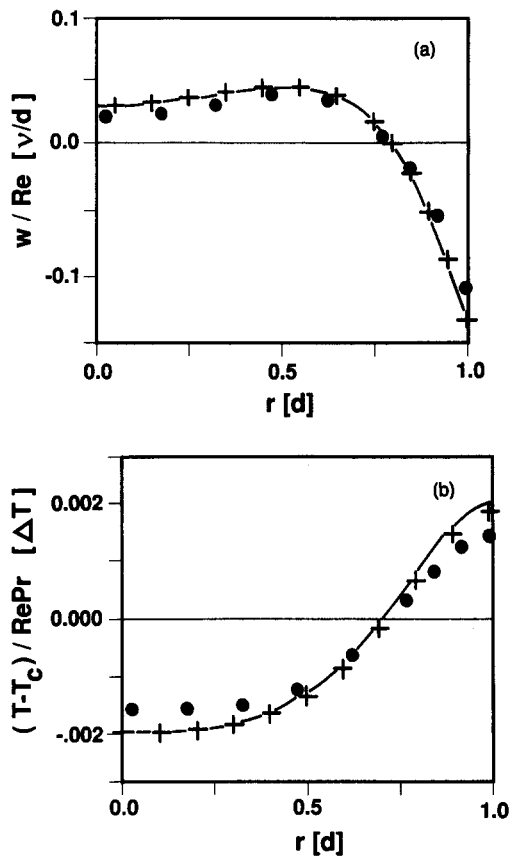


FIG. 2. Radial dependence of (a) axial velocity  $w(r)$  and (b) temperature  $T(r)$  at midplane  $z = 0$  for  $\Gamma = 1$ ,  $\text{Pr} = 0.1$ , and  $C = B = \text{Gr} = 0$ . Full lines represent  $w_{100}$  and  $\theta_{110}$  truncated at  $N = K = 20$ . Pluses and dots are results of a numerical integration<sup>26</sup> for  $\text{Re} = 100$  and  $\text{Re} = 500$ , respectively.

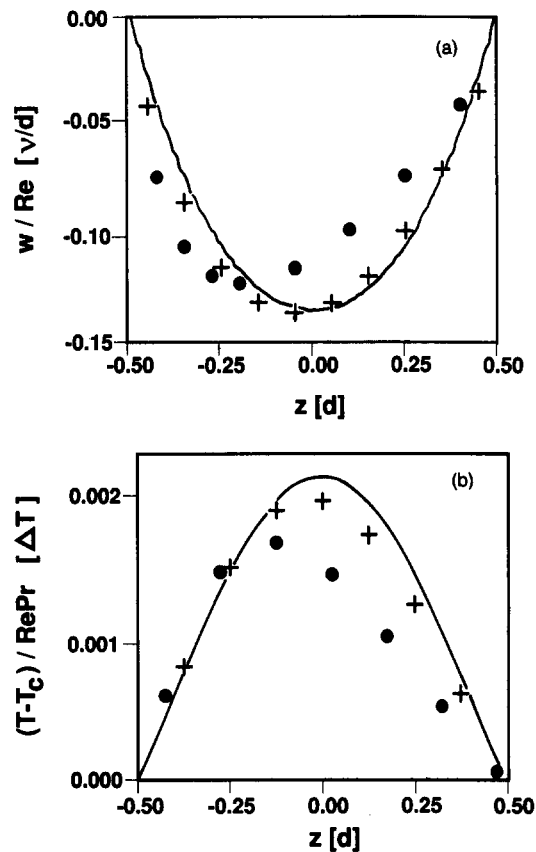


FIG. 3. Axial dependence of (a) axial velocity  $w(z)$  and (b) temperature  $T(z)$  at the free surface  $r = 1/\Gamma$ . Parameters and symbols as in Fig. 2.

is shown in Figs. 2(a) and 2(b) for  $\Gamma = 1$ ,  $\text{Pr} = 0.1$ ,  $B = 0$ , and  $\text{Gr} = 0$ . The results from the present theory and numerical simulation<sup>26</sup> are nearly identical for Reynolds numbers as large as 100. For larger Reynolds numbers, the present approximation loses its validity as indicated by the numerical result for  $\text{Re} = 500$  [dots in Figs. 2(a) and 2(b)]. The axial dependence of  $w$  and  $T$  shown in Figs. 3(a) and 3(b) for the same set of parameters is more sensitive. Even for  $\text{Re} = 100$  the numerical data are slightly asymmetric. The asymmetry of the flow at  $\text{Re} = 500$  results from a combined inertia effect<sup>27</sup> of  $O(\text{Re}^2)$  and thermal coupling at the free surface at  $O(\text{Re}^2 \text{Pr}^1)$ . The latter gets notably smaller if  $\text{Pr} < 0.1$ , thus improving the approximation. The degree of asymmetry in the numerical results decreases with increasing  $\Gamma$ . This is seen in Fig. 4, where the axial velocity on the free surface  $r = 1/\Gamma$  is shown for  $\Gamma = 5$ ,  $B = 0$ ,  $\text{Gr} = 0$ , and  $\text{Pr} = 0.1$ . Small deviations from the numerical results occur only for  $\text{Re} = 500$  in the region  $z \lesssim 0$ . In a large range around the midplane  $z = 0$ , the surface velocity has already taken the value for the infinitely long system<sup>14</sup> ( $w/\text{Re} = -1/4\Gamma = -0.05$ ). Note that  $\theta(r = 1/\Gamma)$  vanishes as  $\Gamma \rightarrow \infty$ .

Modification  $\theta_{110}$  to the conduction temperature field caused by a nonzero heat transfer coefficient  $B$  are in good agreement with the numerical simulation as long as  $\text{Re} \lesssim 200$ . Grashof number effects entering the velocity field at  $O(\text{Re} \text{Pr})$  are not studied here because of the lengthy ex-

pressions involved. The choice of a linear gas temperature  $T_a(z)$  has been made for simplicity. However, the above method can be easily applied to other heating profiles, which, if they are smooth enough, may lead to even better convergence of  $\psi_{100}$  and  $\theta_{110}$ .

The analytical solutions for small  $\text{Re}$ ,  $\text{Pr}$ , and  $C$  capillary flow in a liquid bridge given here are good approximations for a wide range of Reynolds numbers. They may serve

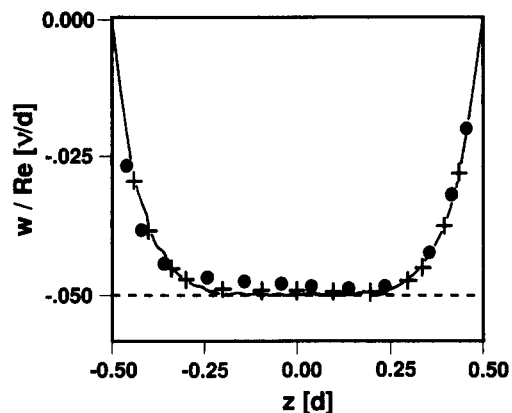


FIG. 4. Axial variation of the axial velocity  $w(z)$  at the free surface  $r = 1/\Gamma$  for  $\Gamma = 5$ ,  $\text{Pr} = 0.1$ ,  $C = B = \text{Gr} = 0$ . The straight line is  $w_{100}$  with  $N = 80$ , the dashed line is the solution for  $\Gamma \rightarrow \infty$ ,<sup>14</sup> and pluses and dots are numerical results<sup>26</sup> for  $\text{Re} = 100$  and  $\text{Re} = 500$ , respectively.

as reference solutions, which can be easily computed to any desired precision. It is not sure, on the other hand, if these solutions can be used in place of the exact basic steady flow in modeling its instability and the onset of low Prandtl number time dependent thermocapillary convection; no models have been given yet. However, since the strength of the exact basic velocity field is essentially linear in  $Re$ , and asymmetries in  $\psi$  result from thermal coupling are small for large aspect ratios and  $Gr = 0$ , one might hope that the instability mechanism and the amplitude of oscillatory thermocapillary convection can be reasonably well described on the basis of the above approximation.

#### ACKNOWLEDGMENTS

The author acknowledges discussions with G. P. Neitzel and A. Benmalek, and thanks Y. H. Shen and D. F. Janowski for providing their numerical data.

This work was supported by the Alexander von Humboldt Foundation and the National Science Foundation.

<sup>1</sup>For a review, see S. Ostrach, *J. Fluids Eng.* **105**, 5 (1983).

<sup>2</sup>D. Schwabe, A. Scharmann, F. Preisser, and R. Oeder, *J. Cryst. Growth*

**43**, 305 (1978).

<sup>3</sup>C.-H. Chun and W. Wuest, *Acta Astronaut.* **5**, 681 (1978).

<sup>4</sup>F. Preisser, D. Schwabe, and A. Scharmann, *J. Fluid Mech.* **126**, 545 (1983).

<sup>5</sup>P. A. Clark and W. R. Wilcox, *J. Cryst. Growth* **50**, 461 (1980).

<sup>6</sup>B.-I. Fu and S. Ostrach, *Transport Phenomena in Materials Processing* (ASME, New York, 1983).

<sup>7</sup>C. Cuvelier and J. M. Driessen, *J. Fluid Mech.* **169**, 1 (1986).

<sup>8</sup>A. Rybicki and J. M. Floryan, *Phys. Fluids* **30**, 1956 (1987).

<sup>9</sup>A. Rybicki and J. M. Floryan, *Phys. Fluids* **30**, 1973 (1987).

<sup>10</sup>H. F. Bauer, *Z. Flugwiss. Weltraumforsch.* **6**, 252 (1982).

<sup>11</sup>M. K. Smith and S. H. Davis, *J. Fluid Mech.* **132**, 119 (1983).

<sup>12</sup>M. K. Smith and S. H. Davis, *J. Fluid Mech.* **132**, 145 (1983).

<sup>13</sup>A. K. Sen and S. H. Davis, *J. Fluid Mech.* **121**, 163 (1982).

<sup>14</sup>J.-J. Xu and S. H. Davis, *Phys. Fluids* **26**, 2880 (1983).

<sup>15</sup>J.-J. Xu and S. H. Davis, *Phys. Fluids* **27**, 1102 (1984).

<sup>16</sup>M. K. Smith, *Phys. Fluids* **29**, 3182 (1986).

<sup>17</sup>R. C. T. Smith, *Aust. J. Sci. Res.* **5**, 227 (1952).

<sup>18</sup>D. D. Joseph and L. Sturges, *J. Fluid Mech.* **69**, 565 (1975).

<sup>19</sup>J. Y. Yoo and D. D. Joseph, *SIAM J. Appl. Math.* **34**, 247 (1978).

<sup>20</sup>A. Benmalek, M.S. thesis, University of Bristol, 1987 (unpublished).

<sup>21</sup>C. I. Robbins and R. C. T. Smith, *Philos. Mag.* **39**, 1004 (1948).

<sup>22</sup>H. K. Moffatt, *J. Fluid Mech.* **18**, 1 (1964).

<sup>23</sup>J.-J. Xu and S. H. Davis, *J. Fluid Mech.* **161**, 1 (1985).

<sup>24</sup>D. D. Joseph, *SIAM J. Appl. Math.* **33**, 337 (1977).

<sup>25</sup>D. D. Joseph and L. Sturges, *SIAM J. Appl. Math.* **34**, 7 (1978).

<sup>26</sup>Y. H. Shen, Ph.D. thesis, Arizona State University, 1989 (unpublished).

<sup>27</sup>O. R. Burggraf, *J. Fluid Mech.* **24**, 113 (1966).